Methodology for Flow and Salinity Estimates in the Sacramento-San Joaquin Delta and Suisun Marsh

33rd Annual Progress Report
June 2012

Chapter 6
A Continuous Surface Elevation Map for Modeling

Authors: Rueen-Fang Wang and Eli Ateljevich
Delta Modeling Section
Bay-Delta Office
California Department of Water Resources

Page left blank for two-sided printing

Contents

Figures

Page left blank for two-sided printing

6 A Continuous Surface Elevation Map for Modeling

6.1 Introduction

Bed elevation is an important input to any hydrodynamics model, and the Delta Modeling Section has maintained a database of bathymetry soundings and levee surveys for decades. In recent years, new data have become available; technology has shifted to very dense multibeam sonar soundings; and the demands on accuracy have increased due to increasingly common multidimensional modeling of the region. In some locations, such as near the Burlington Northern Santa Fe (BNSF) Railway Bridge shown in Figure 6-1, newer elevation data differ from earlier elevation models by as much as 50% to 100%. The differences can be due to evolution of the bed, improved sounding, and georeferencing techniques, or denser coverage of areas that were previously interpolated.

This chapter documents the development of an elevation data set for multidimensional modeling developed under the REALM project, synthesizing LiDAR, single- and multibeam sonar soundings and surveys and integrating them with existing integrated maps that themselves were collated from multiple sources.

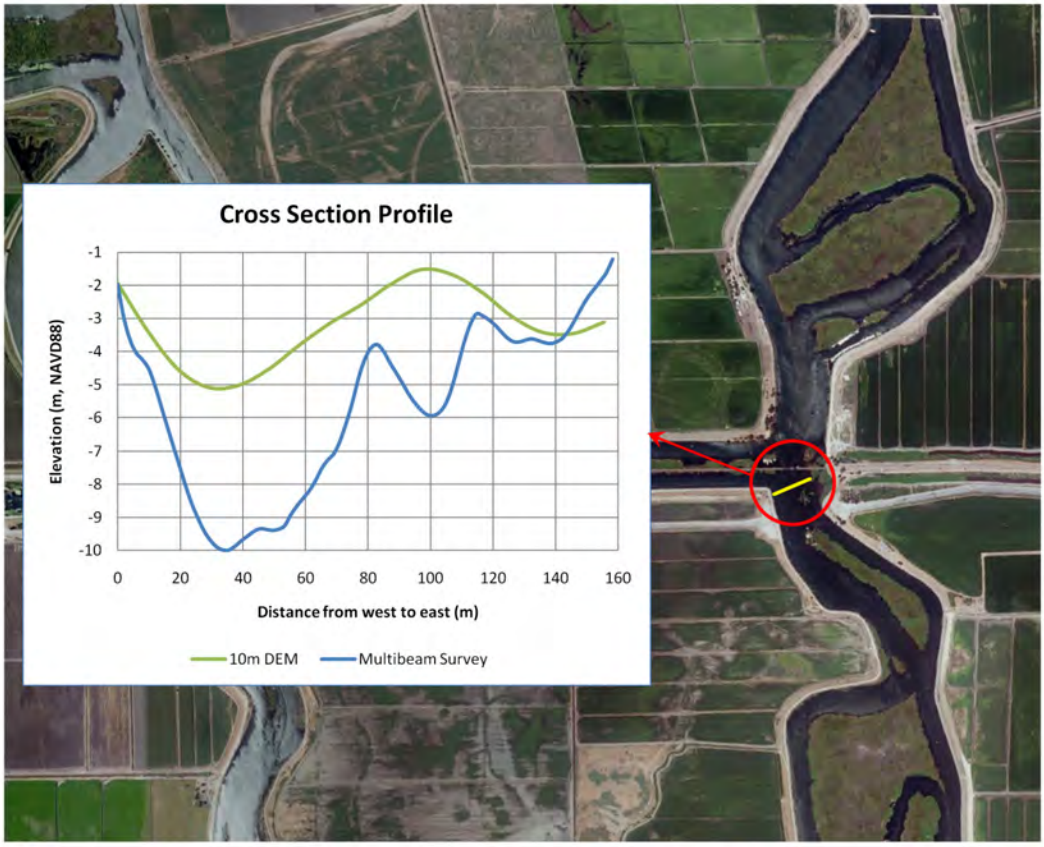

Figure note: DWR Central District shows the magnitude of the discrepancy between older (green, 10 m Digital Elevation Map [DEM]) elevations data and more recent high resolution (blue, Multibeam Survey) soundings. The region is near a bridge abutment, but the magnitude of discrepancy is typical of the stretch of Middle River for several kilometers south.

Figure 6-1 Cross Section Profile near BNSF Railway Bridge

The result is a continuous surface—terrestrial and water—in meters using the NAVD88 vertical datum. The initial release of this map was in the form of a 10 m Digital Elevation Map (DEM) for the entire Bay-Delta and parts of the coast to the Farallones, supplemented by a 2 m model of the South Delta in a region where the channel features are poorly resolved at 10 m. These data are raster data sets, meaning they are defined on a rectangular mesh with square cells, some of which may be declared missing. Raster data are compatible with data formats used for modeling and allow a greater variety of Geographical Information System (GIS) analysis. However, in regions where high resolution LiDAR and multibeam coincide, we are moving some of our analysis to ArcGIS Terrain data sets. A Terrain is a collection of dense points, lines, and polygons. It is a form of data that makes good use of disparate data and is efficient for huge clusters of points. However, it is a proprietary data structure not directly usable by hydrodynamic models.

One requirement of the project is to always have a product and to release updates as frequently as 2 times per year. During each release, the products are essentially rebuilt from the base maps, adding newer data sets on top of the old in a systematic way. Users of the map are urged to join an issue tracking system, as the faults they find are addressed in each iteration.

The remainder of this chapter outlines the data sources we use for the project, the method of preparation, and challenges involving both data and modeling applications. Only modest attention is given to a traditional subject: interpolation. In the course of the project, we have made use of promising, robust interpolators to fill gaps when there is supporting data (hand soundings and digitized photos). However, we are concerned about spending too much effort near the point of decreasing returns. The newer bathymetric and LiDAR data present a dichotomy between data that is either very dense or is entirely missing, and it is hard to increase the information content in a gap under those circumstances.

6.2 Data Sources

The work presented here is based largely on elevation models, which themselves were stitched together from multiple sources. Figure 6-2 shows the core data, comprising mainly DWR LiDAR (Dudas, 2010), the Foxgrover 10 m bathymetry in the Delta (Foxgrover, Smith, & Jaffe, 2003) and the NOAA San Francisco Bay DEM (Carignan, et al., 2010). Some outlying regions are covered only by the USGS National Elevation Dataset (http://ned.usgs.gov/)—the NED data are less accurate and congruent with the other data, but are only employed in places that are fairly remote from tidal water bodies. The figure also shows additional point data sets that were incorporated in Version 1. Most are single beam soundings (DWR, Towill, Inc. 2009, and CSDP bathymetry data, online), but some are hand digitized contour maps (Smith). The DEM for the San Joaquin River near Vernalis is created based on the 1988 COE survey (CSDP bathymetry data, online). The transects for this survey were closely spaced and realistic; but due to morphological changes, the data had to be manipulated ("rubbersheeted") to coincide with the recent channel bed. The 2 m South Delta also contains a modest number of synthetic points estimated along channel centerlines. This 2 m effort was undertaken not so much because the data at the time justified it in all places, but rather because we believe that certain locations in the South Delta are too narrow to be represented at 10 m. Resolution of elevation maps for modeling is discussed later.

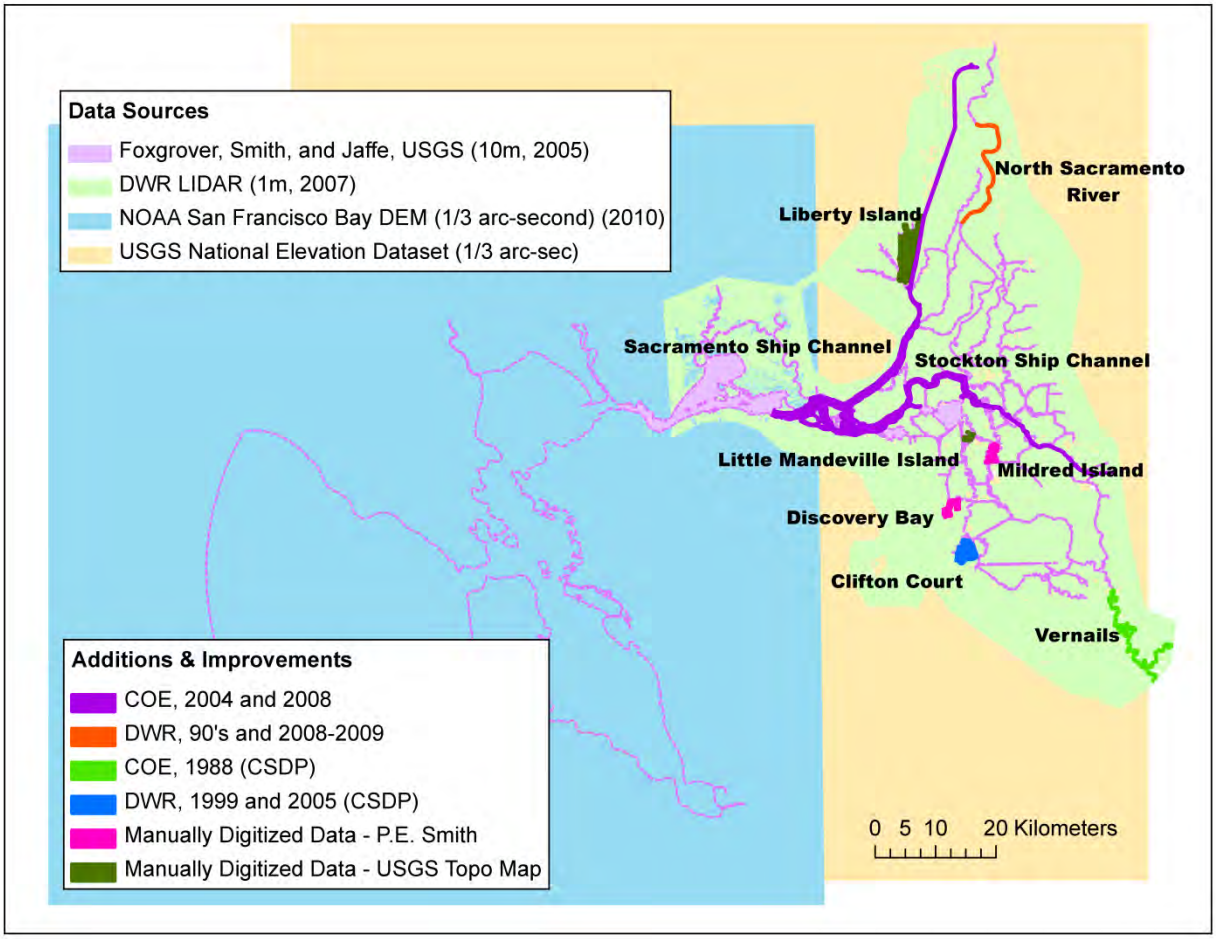

Figure note: References for data sources in version 1.0 DEM:

Foxgrover, Smith, and Jaffe, USGS (10m, 2005)	Foxgrover, Smith, & Jaffe, 2003
DWR LiDAR (1m, 2007)	Dudas, 2010
NOAA San Francisco Bay DEM (1/3 arc-second) (2010)	Carignan, et al., 2010
USGS National Elevation Dataset (1/3 arc-sec)	http://ned.usgs.gov/
COE, 2004 and 2008	Towill, Inc., 2009
DWR, 90's and 2008-2009	DWR
COE, 1988 (CSDP)	CSDP bathymetry data (online)
DWR, 1999 and 2005 (CSDP)	CSDP bathymetry data (online)
Manually Digitized Data - P.E. Smith	Smith
Manually Digitized Data - USGS Topo Map	http://services.arcgisonline.com/arcgis/services

Figure 6-2 Data Sources for Version 1.0 of the 10 m DEM

Version 2 of the elevation model is being prepared and is slated for release in late summer 2012. For the new version, a number of additional high resolution data sets have been identified and are being vetted for inclusion. Figure 6-3 shows a map of these data sets. The updates are being prepared as a set of discrete 2 m "patches" on the base map. Most of the data for Version 2 are multibeam or exceptionally high resolution single beam observations.

Finally, we expect a round of enhancements to be released in each of our base data sets. The USGS is currently creating a 2 m DEM including both terrestrial and soundings data. DWR is creating an

enhanced release of the terrestrial Delta LiDAR data set that solves some interpolation and missing data issues with the original release.

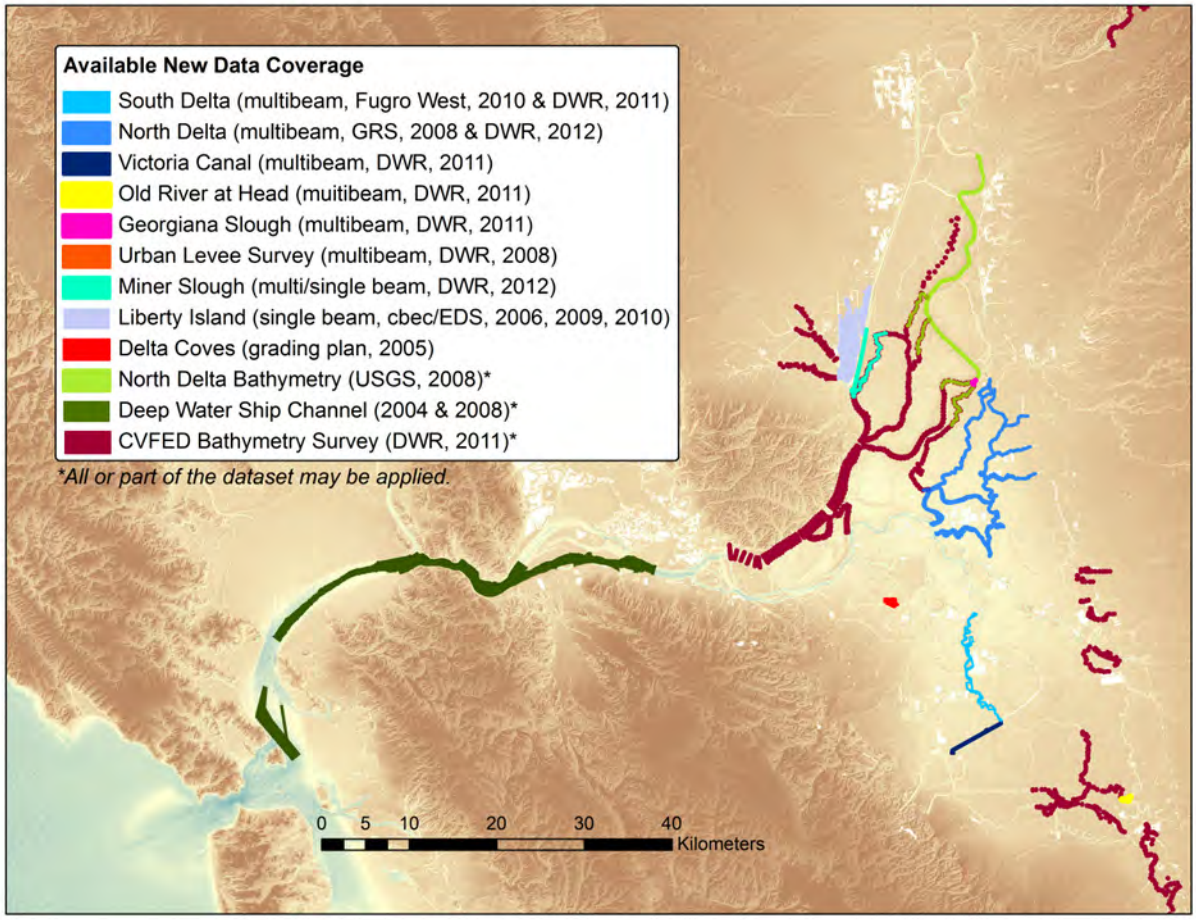

Figure note: References for the available new data:

South Delta (multibeam, Fugro West, 2010 & DWR, 2011)	(Mayr, 2011), (Fugro West, Inc., 2008)
North Delta (multibeam, GRS, 2008 & DWR, 2012)	(GRS, 2008), Mayr, 2011-2010
Victoria Canal (multibeam, DWR, 2011)	(Mayr, 2011)
Old River at Head (multibeam, DWR, 2011)	Mayr, 2011-2012
Georgiana Slough (multibeam, DWR, 2011)	Mayr, 2011-2012
Urban Levee Survey (multibeam, DWR, 2008)	(Fugro West, Inc., 2008)
Miner Slough (multi/single beam, DWR, 2012)	Mayr, 2011-2012
Liberty Island (single beam, cbec/EDS, 2006, 2009, 2010)	(EDS, 2006), (EDS, 2009), (Campbell, 2012)
Delta Coves (grading plan, 2005)	(Ruggeri-Jensen-Azar & Associates, 2005)
North Delta Bathymetry (USGS, 2008)	(USGS, 2008)
Deep Water Ship Channel (2004, 2008)	(Towill, Inc., 2009)
CVFED Bathymetry Survey (DWR, 2011)	(HDR, 2011); (PBS&J, An Atkins Company, 2010)

Figure 6-3 Data Sources Being Added for Version 2.0 of Elevation Model

6.3 Methodology Overview

Before outlining the methodology of preparation, it is useful to reiterate the end products. We produce a 10 m DEM everywhere plus 2 m standalone point or raster models of special focus regions such as the South Delta. The finer DEM is obtained from a terrain model. In the process of preparing the 2 m patch, the background 10 m model is improved and edge-matched to the 2 m data.

6.4 10 m Base Map

The method for producing the 10 m map is shown in Figure 6-4. The main steps are discussed below.

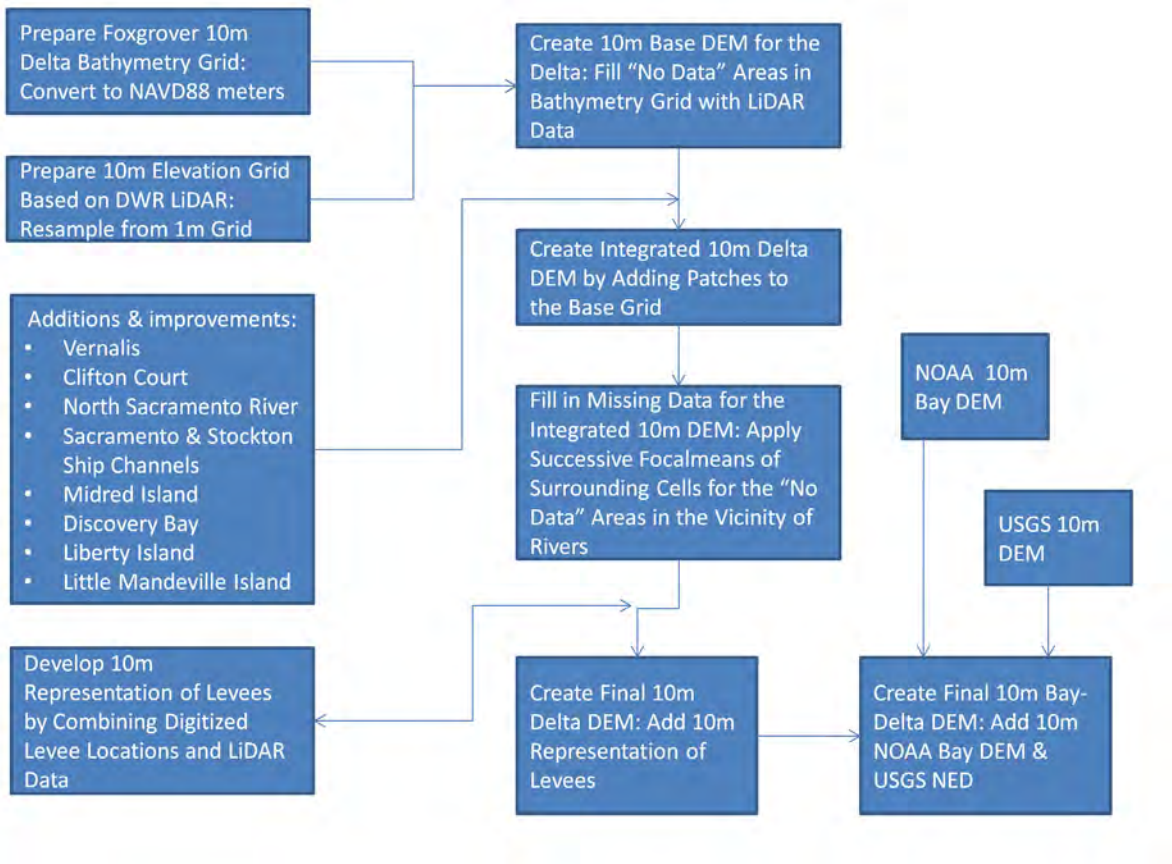

Figure 6-4 Preparation of 10 m DEM

6.4.1 Prioritization of Core Data and Supplemental Data Sets

To reconcile the base data, LiDAR is resampled or interpolated to a common 10 m grid, the bathymetry and LiDAR are overlain, and overlapping regions are determined by priority. In Version 1, we prioritized the bathymetry over terrestrial data; and we continue to do this for our 2 m maps. But in Version 2, we are prioritizing terrestrial data at 10 m.

The additional low-medium resolution data listed in Figure 6-2 then nested within the 10 m grid. In Version 1, the ArcGIS topo-raster was used in most places to complete a raster where point data were sufficiently dense. Topo-raster is a thin plate spline with enforcement of contours and drainage directions frequently used with hydrologic features.

6.4.2 Filling at 10 m and Missing Values

Both LiDAR and our base bathymetry maps contain missing data; and because neither captures the shoreline reliably, there is a gap between them. Where gaps and missing values can be appropriately filled, successive applications of kernel averages (*focal means* in ArcGIS) were used to fill holes from the edges in—each new kernel average would fill one new cell working toward the interior of the "hole" in the data, a technique we are currently reconsidering. Missing regions remote from water were left missing. No large regions in the Delta were left without some form of estimate, mostly because the Foxgrover 10 m DEM itself contains a lot of estimated data and fill values which we left intact. In some cases with missing LiDAR returns, we had little basis for guesses besides what we could see from aerial photos.

Most remaining missing values are on land, and some are behind levees. Although it is certainly not an infallible generalization, users who need to fill the remaining missing data in our model should use a mild dry elevation above the threshold of sea level rise (we often use 8 m, NAVD).

6.4.3 Transitions between Data Sources

Except for the LiDAR, data sources informing the 10 m map are not highly accurate and were collected over the course of decades. There is no guarantee of smoothness between them, and discontinuities occasionally occur at transitions. We fixed the transitions by hand, using local kernel averages to smooth the map. The transition zone over which we smooth is approximately 100 m.

6.4.4 Orthogonal Levee Reinforcement

One of the hazards of an integrated 10 m land-water elevation model is that the width of a levee crest is slightly under-resolved. And some aspect of the sampling or data processing can cause a low-lying raster cell to develop along a narrow levee crest, creating a false numerical "leak" in the elevation model between channels and islands. Such a numerical leak is shown in Figure 6-5 and is more common when the levee runs at an angle to the raster.

The levee refinement problem goes away when the data are finer. Levee crests are always well resolved by 2 m data. We enforce them in the 10 m model by reference to the finer data:

1. Levees are digitized into a vector (line) feature.
2. 10 m and 2 m raster cells are identified that intersect the levee.
3. The 10 m cells are set to the maximum of
   a. their own value or
   b. the elevation of the highest 2 m cell inside the 10 m cell that also intersects the levee.

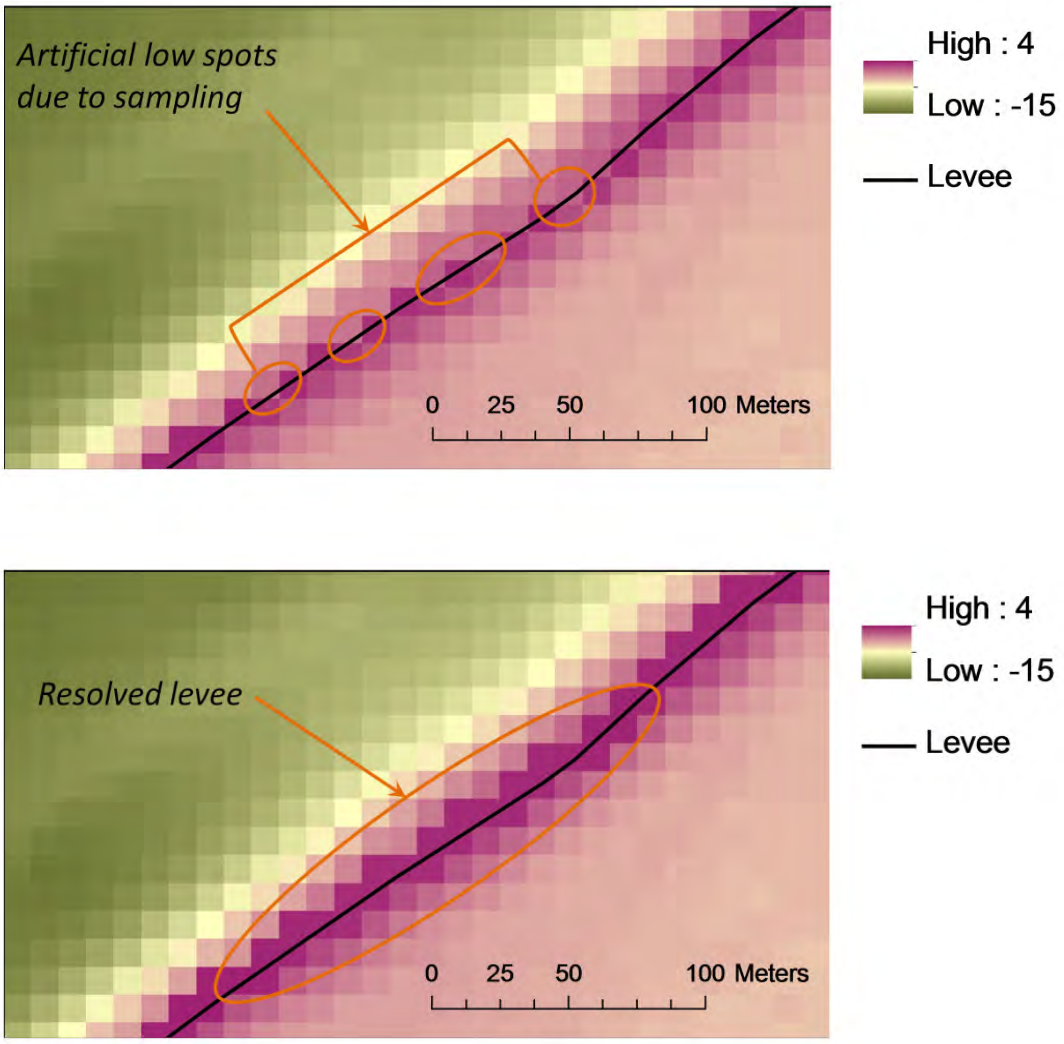

Figure note: (Top) Levees with artificial low spots in the elevation model due to coarse sampling. (Bottom) Orthogonal reinforcement of levees using finer data so that the levees do not have low spots in the elevation model.

Figure 6-5 Examples of False Numerical 'Leaks' in Levee Elevation Models

6.5 High Resolution Model

In Version 2, we have begun to introduce 2 m high resolution patches where LiDAR and dense (often multibeam) data coincide. The patches have value as standalone products, though the usefulness of data at this resolution for modeling should not go unquestioned; and we assume that users of the finer data are acquainted with the sampling issues raised at the end of the chapter.

The finer data are prepared using their own fill techniques. The nominal vertical accuracy of the soundings and terrestrial data is submeter—hence the accuracy of the 2 m patch is determined for the most point by the size and complexity of the gaps between them.

6.5.1 Gaps

The most vexing issue that arises in deriving a continuous surface model is that the land-base LiDAR and water-based soundings do not meet. The shoreline determines the tidal prism, and its width is arguably one of the most critical parameters for modeling. There is also often an abrupt change in slope near the interface between land and water, and the change is almost never observed or resolved. In channels, the region of missing data is routinely 10 to 20 m wide, but the gap can be much larger for islands with poor LiDAR returns or in shallows that are not navigable by boats collecting multibeam soundings.

Our approach is to categorize the gaps according to nature and complexity and to apply a simple and automatable method for gaps that are narrow and tractable. We have methods to treat the special cases depending on the width of the gap, the complexity of the water body, available supporting data such as hand soundings or prior collections and which data source (land or water) is causing the gap. We also prune away the hardest gaps when interpolation seems to compromise most of the benefits of updating the data.

6.5.1.1 Simple Gaps

A typical case is shown in Figure 6-6 where a narrow sliver of missing data 10 to 40 m wide separates the land and water data on either side of a small island near the junction of Victoria Canal and Old River. A 3-segment transect is indicated crossing both sides of the island where we performed a comparison of interpolants. An abrupt slope change exists on 2 of the 4 banks (this is more apparent in Figure 6-7), and trying to fit the break in slope is the only technical challenge. We have indicated the apparent location of the shore according to aerial photos. The images available to us are vague and shadowy, but we believe our guess is accurate to ± 5 to 15 m laterally.

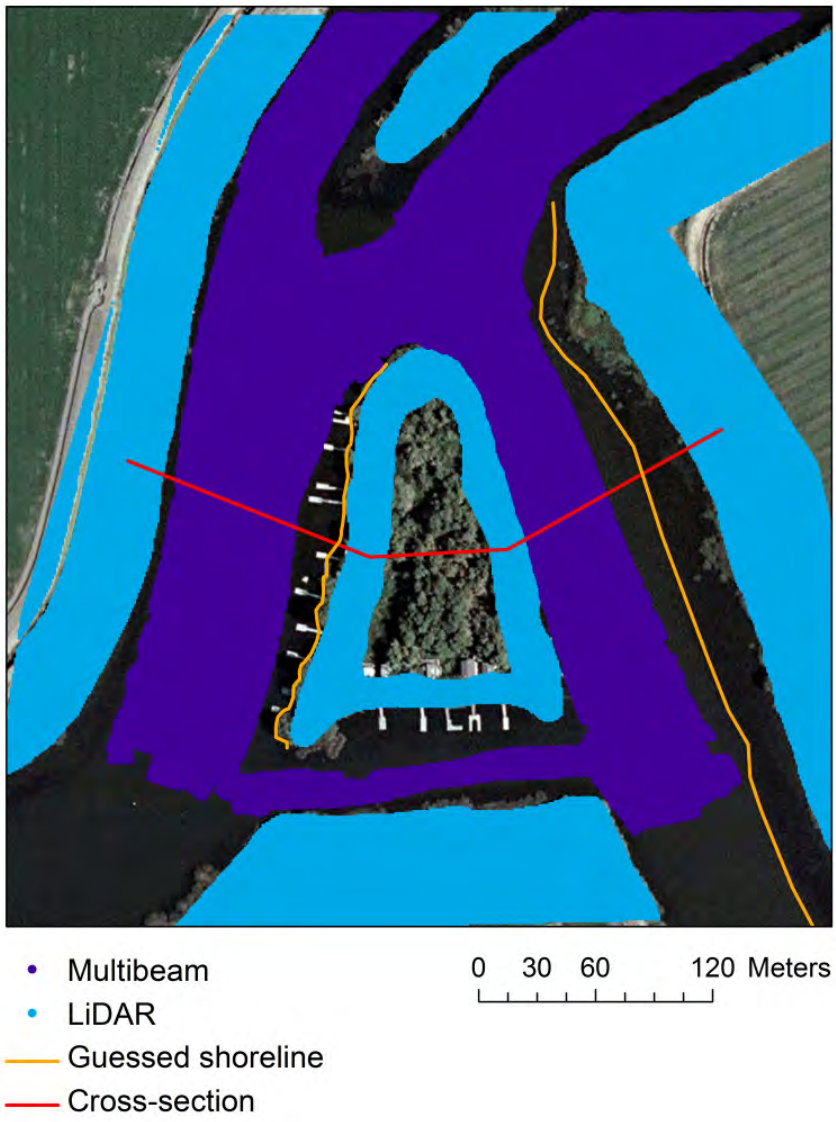

Figure note. Simple gaps between multibeam (purple) and LiDAR (blue). A bent transect used for interpolation comparisons is shown in red.

Figure 6-6 Example of Simple Gaps

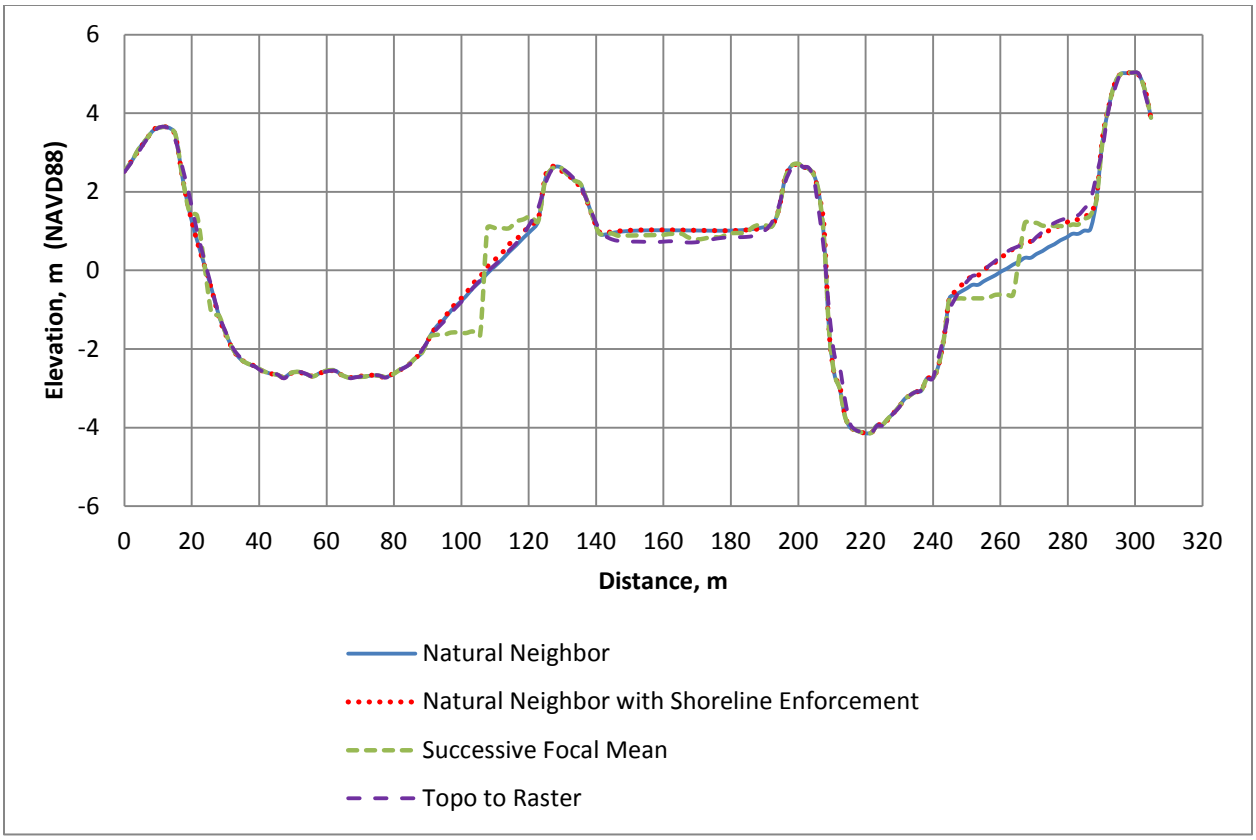

Figure 6-7 Comparison of Interpolation Techniques on Simple Gap

Figure 6-7 shows a vertical profile along the red transect in Figure 6-6 given by several different interpolants:

1. natural neighbor;
2. natural neighbor with reinforcement of a guess (0.75 m NAVD) at the shoreline from photos;
3. successive application of kernel averages (*focal means* in ArcGIS) in no data areas from the outside in;
4. thin plate splines using topo-raster, a method that handles a small amount of local anisotropy in the streamwise and cross-stream direction.

With the exception of successive focal means, there is little to distinguish the methods. The interpolants all resolve the fairly continuous shore gradients near 20 m and 210 m, and they all suffer from the missing data and ambiguous gradients at 100 m and 260 m. Methods (1) and (2) are particularly economical, as they can be applied automatically when converting data from ArcTerrain data sets to 2 m raster. Method (3) seemed successful and expedient on coarser 10 m data where the gaps were only 1 to 2 raster cells wide. It produces a discontinuity in the middle of the gap that tends to force inundated area to a medium value, but it also looks odd at higher resolutions. As with most thin plate and many other families of interpolants, method (4) is known to work well near data that are well balanced in resolution—where the smallest and largest gaps between data are not very different. This assumption is violated here—but perhaps more important to us, topo-raster is designed for smaller data structures and requires more processing for dense terrain data.

6.5.1.2 Missed Returns on Islands

One of the most common large-gap cases occurs when berms and islands go entirely or partially missing in the LiDAR returns. This is common in split channels such as Victoria Canal, and as in the previous example we assume the slope of the bathymetry gives no accurate indication of the slope of the land. In this case our goal is to plausibly fill the water portion and set the island to a missing value that we hope the user will fill using a mild "dry" value. To achieve this result, we digitize the shoreline as a (hard) line feature or breakline in our Terrain model and assign it a locally average elevation—the guess at which may be aided by any patches of non-missing LiDAR. In Figure 6-8, the perimeter of the island is delineated by a polygon—the island itself had no LiDAR returns.

Figure 6-8 Delineation of an Inhabited Island Using Bounds of a Polygon as a Hard Constraint

For our assumed shoreline, we generally choose a value that represents a locally near-mean tidal surface to represent the digitized shore. For instance in the South Delta, this might be 1.0 to 1.5 m NAVD88—the number is based on an informal analysis. Because the enforced shoreline is assigned based on photos taken at an unknown point in the tide cycle, the absolute accuracy of this method at the shore can never be better than the tidal amplitude, or about ± 0.5 to1.0 m. However, the approximation has good qualitative properties: The slope will be accurate (near zero) along the shore,

and the inundated area around small islands is more correct. Figure 6-9 shows how useful island enforcement is in preserving inundated area—the (blue solid) unenforced case simply interpolates from bathymetry to LiDAR, inundating a small community and overestimating the extent of the tidal prism by a large amount.

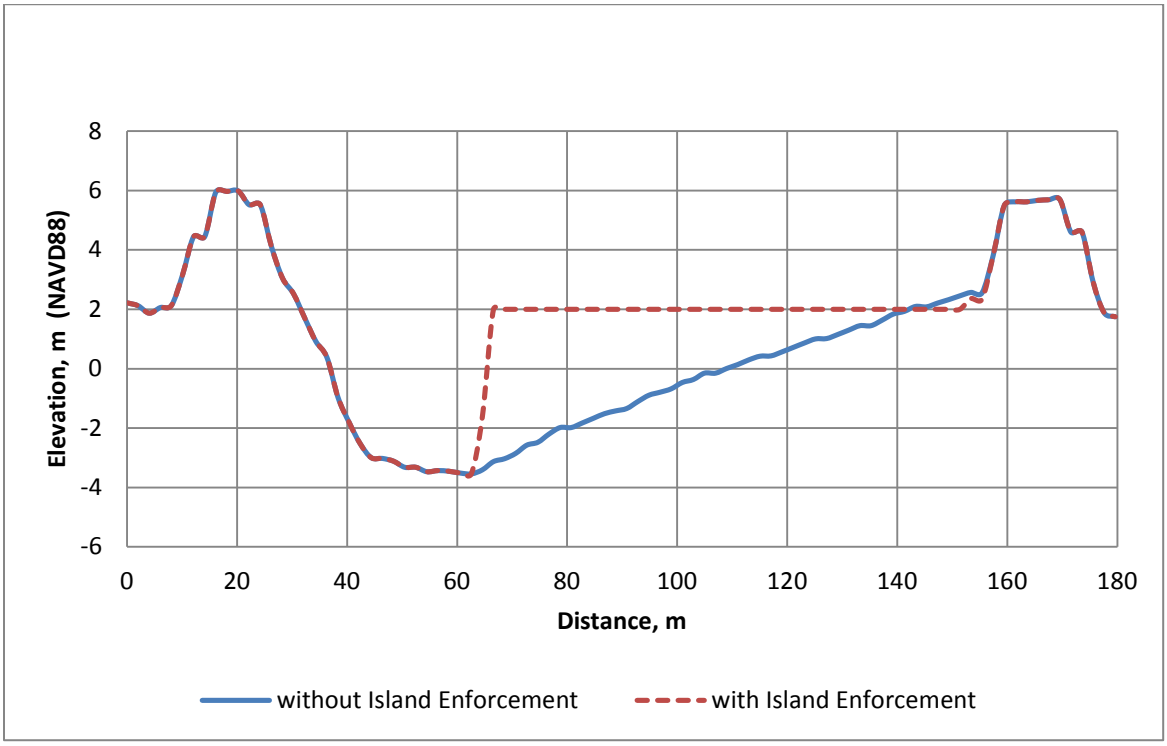

Figure 6-9 Cross Section Profiles with and without Island Enforcement

6.5.1.3 Complex Shallows

A catch-all category for regions that interpolate poorly filled, complex gaps often occur at the fringes of a multibeam collection or in regions where the multibeam collection misses impassible shallows. The issue often coincides with berms and complex geometry around small islands, in which case the LiDAR returns can be missing as well. Our goal in this case is to plausibly fill the water portion of the data and to fill the land if it is adequately represented by LiDAR returns. Whether we are able do this accurately enough to salvage or justify a map of the region in 2 m resolution depends on the supporting data—lacking that, we prefer to trim the difficult regions.

Figure 6-10 shows a hydraulically important junction near the BNSF railway crossing on Middle River, which flows north-south from the top to the bottom of the figure. To the west (left in Figure 6-10), the island supporting the railroad is missing LiDAR returns and was treated using the island breakline method from the previous section. To the east, numerous shallow islands have virtually no soundings between them. In this case, the importance of the rest of the data set prompted us to include the new data—but the islands are completely lost except when we use laborious techniques (Wood, Bravington, & Hedley, Soap film smoothing, 2008). And even then, they are not well resolved. To get any sort of reasonable estimate of inundated area, we will need to resample around the islands in the eastern part of the figure.

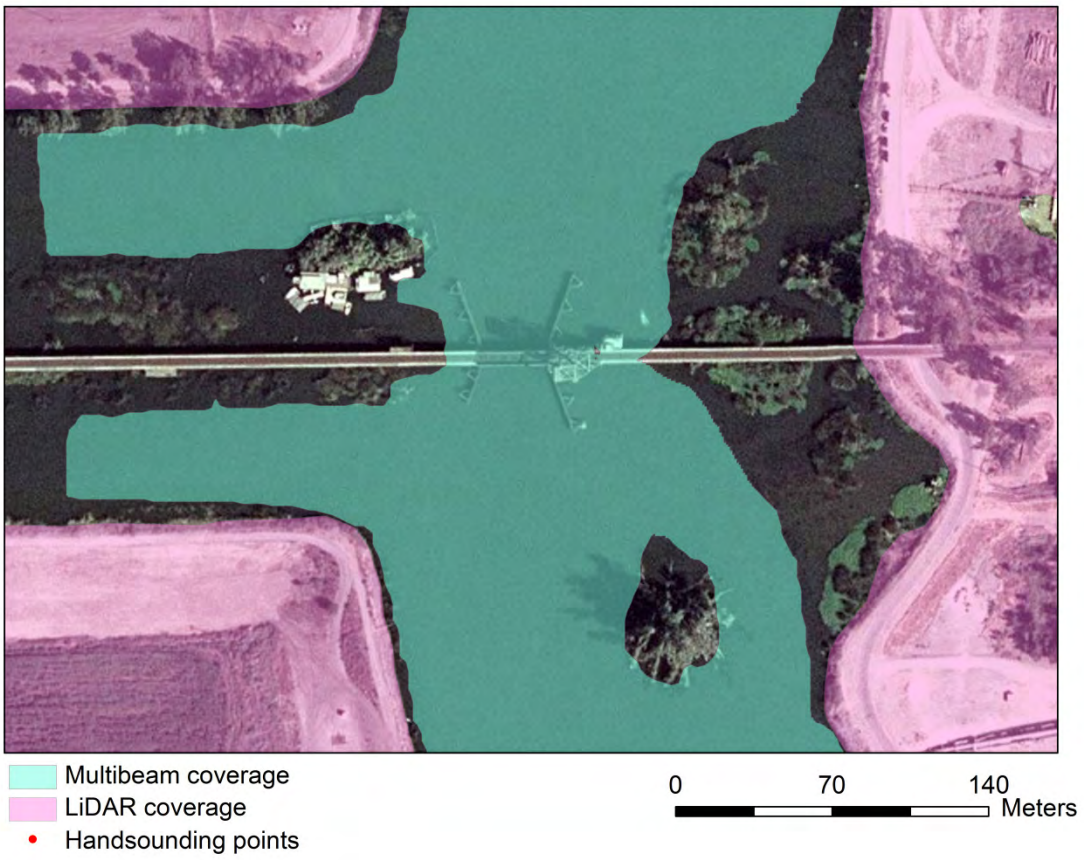

Figure note: The gap in the west side of the figure is due to an island with no LiDAR returns. The gap in the east is more complex, involving shallows, small islands, and structures. In this case, there were few recent hand soundings to support interpolation near the islands.

Figure 6-10 Complex Shallows near BNSF Railroad Bridge Crossing Middle River near Bullfrog Marina

The horseshoe bend in Figure 6-11 is less complex than the railway crossing, but some of it is still too complex and undersampled for out-of-the-box *terrain* interpolation. The region has more auxiliary data than the previous example, including hand soundings and a digitized estimate of the shoreline.

Figure 6-12 shows the improvement in drawing a cross section that can be expected from including supporting data, particularly near the tidal prism. Without supporting data, natural neighbor interpolation gives a nearly straight line fit between the multibeam and LiDAR when there is no shoreline enforcement. However, when a shoreline is imposed as in this example and hand soundings are included, it brings about a 1 m or greater change in vertical elevations and a significantly different characterization of the tidal prism.

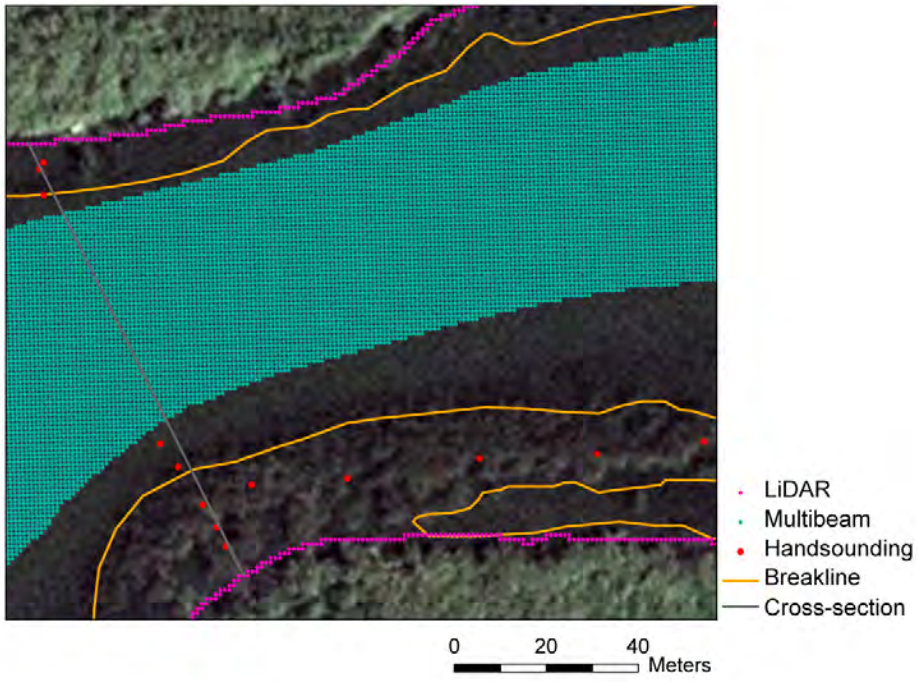

Figure note: Shoreline estimates from photos and locations of some supporting hand soundings are also indicated.

Figure 6-11 Shallow Horseshoe Bend on Middle River North of Bullfrog Marina (top) and Close-up of Southern Part of Bend where Interpolation was Compared (bottom)

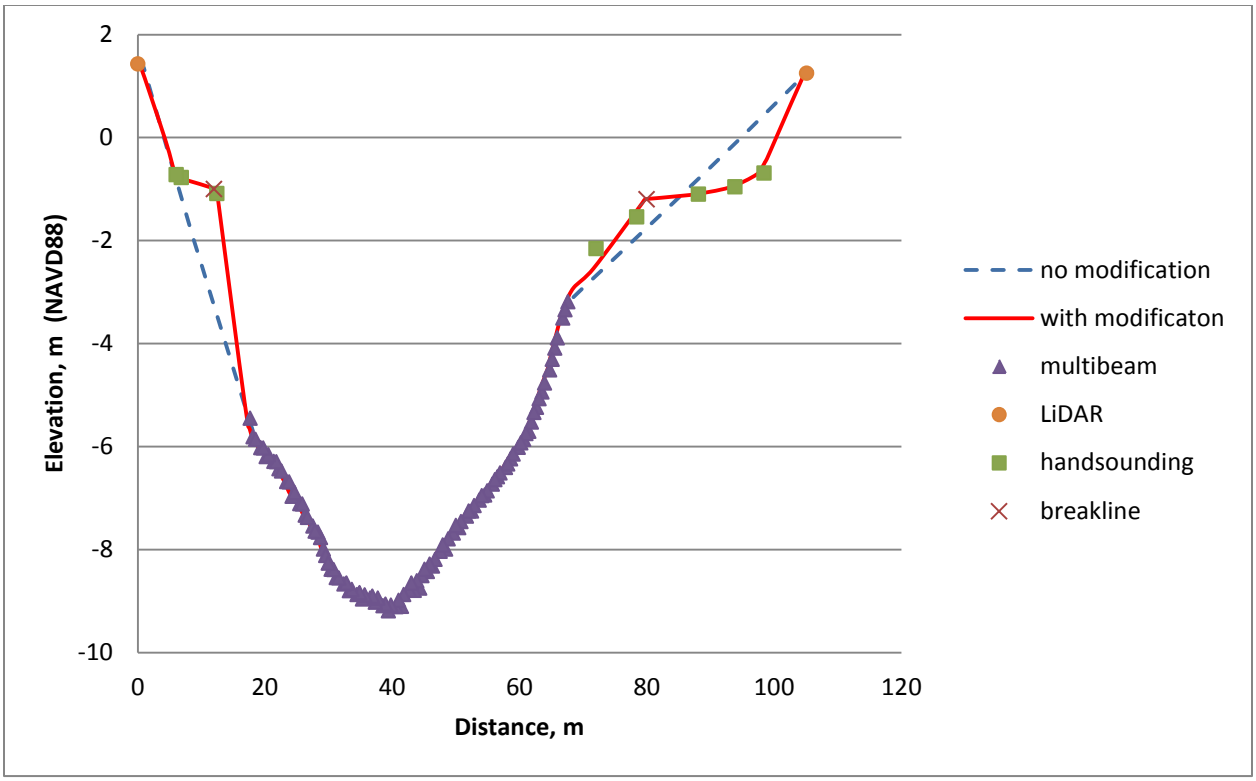

Figure note: Comparison of vertical cross sections on the bend constructed using bathymetry and LiDAR alone (dashed blue) and including hand soundings and hand-drawn breaklines at the shoreline from photography (solid red).

Figure 6-12 Example of Vertical Cross Sections with Supporting Data

Though it makes use of auxiliary data, the fit in Figure 6-12 still comes from a natural neighbor interpolation method that is "out-of-the-box" for an ArcGIS terrain model. When bathymetry is not available, we have to revert to methods that honor boundaries (shores), interpolate realistically, and can robustly handle combinations of fine LiDAR and sparse soundings. In the northern section of the bend, we have been able to fit the channel well qualitatively with multidimensional tensor splines (Wood, 2006) in streamwise and cross-stream coordinates and robustly with soap film smoothers (Wood, Bravington, & Hedley, 2008). Both were implemented in the statistical programming language R. We suspect also that the anisotropic methods of Merwade, Maidment, & Goff (2006) would perform similarly to the tensor splines both in terms of high labor and good performance. However, both methods utilize "streamwise" and "cross-stream" coordinates that are hard to define in many places. We believe that the soap film methods and locally anisotropic methods for shape fitting such as in Casciola, Lazzaro, Montefusco, and Morigi (2005) and (2006) will generalize better to junctions and clusters of islands. We will compare the accuracy and realism of some of these interpolants over complex bathymetry in a future report.

6.6 Fine-coarse Transitions

In a previous section, we noted the possibility of discontinuities between different coarse (10 m) data sources. The same issue arises when 2 m and 10 m products need to agree at their boundaries.

We use the 2 m data to improve the 10 m data locally. Hence, 10 m data that is covered by 2 m data tends to naturally agree with the finer data. The issue is on the border region Figure 6-13. There we created synthetic transitions that allow 2 m and 10 m to nest well. Our goal in this case is that the 2 m

data and underlying 10 m model be left unaltered. The "patching" is done by manipulating the bordering 10 m data within a 100 m distance using successive passes of isotropic kernel smoothers (focal mean) (Figure 6-14).

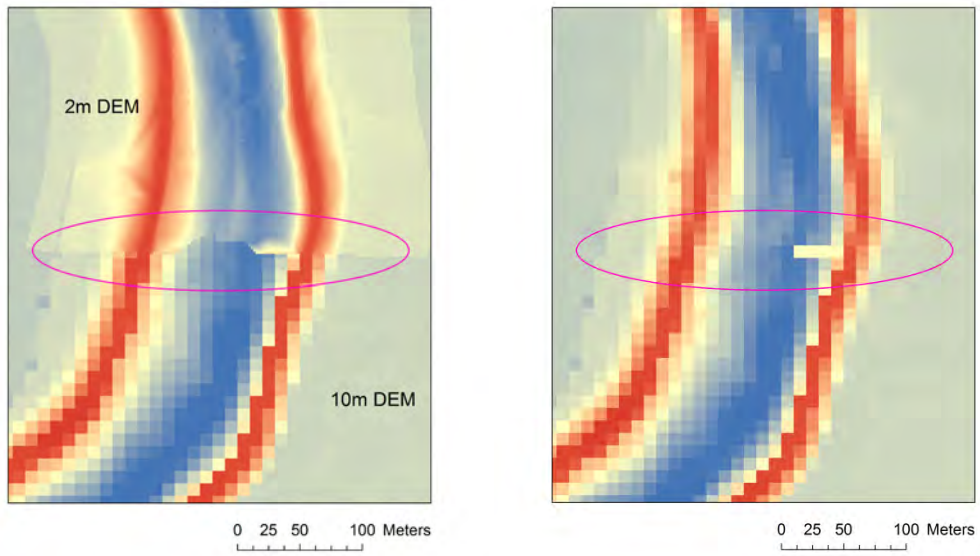

Figure note: (Left) Disagreement at coarse-fine interface between 2 m and 10 m maps. (Right) 10 m map updated using 2 m data with no adjustment at the interface.

Figure 6-13 Example of Fine-coarse Transitions

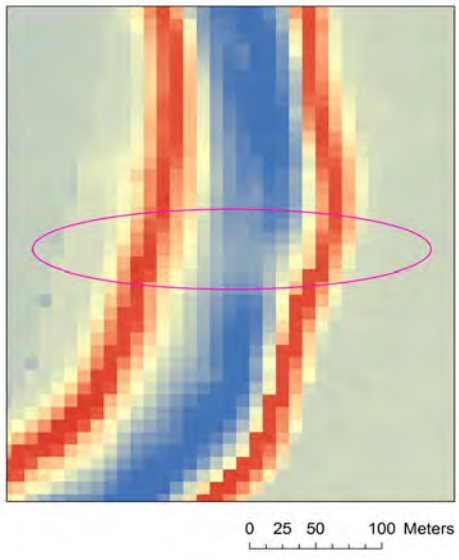

Figure 6-14 Result of Stitching and Smoothing Discontinuity at 10 m

6.7 Time and Spatial Sampling

It is necessary as a modeling assumption to treat an integrated bathymetry map as a synoptic view of the entire domain. In fact, the Delta is constantly changing, including subsidence of land and survey benchmarks, moving bed forms, and morphological change from extreme events. We encountered this evolution in several contexts:

1. **Morphological evolution over decades.** On the San Joaquin River, more than a few kilometers upstream of Old River, only one historical bathymetric survey sampled transects spaced closely enough longitudinally to resolve the channel meanders in the region (approximately 150 m is required, and COE and other institutions have sampling standards much more distant). The one survey available was made in the late 1990s and did not line up with the channel bed suggested by the LiDAR and photos.
2. **Sand wave movement.** Bed forms exist in many areas of the San Francisco Bay and Delta. Relatively few spots have been subject to enough repeated high density monitoring to describe changes over time. Figure 6-15 shows the evolution of sand waves near the Middle River railroad bridge over 3 multibeam surveys that were spaced over 18 months. Within that time, the bed forms appear to evolve and come out of phase with another between the first DWR survey and the Fugo survey; and then the bed forms moved only slightly by the second DWR collection. The absolute difference in elevation at a point between the collections can be over a meter, although there is clearly an "average" bed that is more stable.

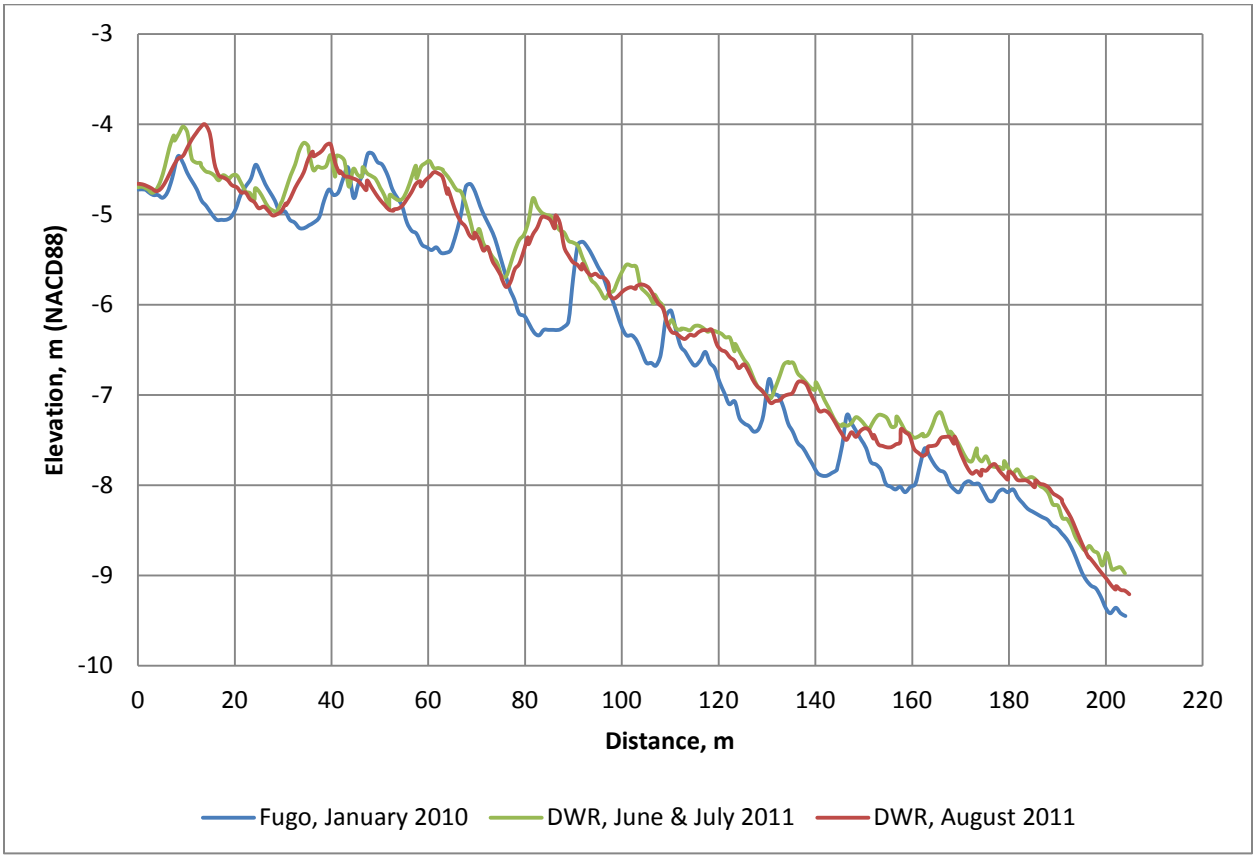

Figure 6-15 Evolution of Channel Bedforms over 3 Data Collections in 2010 and 2011

3. **Methodology discrepancies**. Differences between successive multibeam surveys are almost always interpreted by practitioners as a physical change. The nominal error and precision of the data warrants this, and changes in spatial patterns are often bona fide. On the other hand, errors due to equipment setup and quirks of the day can amount to several tenths of a meter, and the error is often systematic—affecting much of the data collected in one outing in a similar way. It is beyond the scope of this chapter and the available data to quantify this effect. We believe it amounts to between 0.1 m and 0.2 m in the railway bridge region, which is not enough to affect our results.
4. **Spatial sampling goals.** The original LiDAR and multibeam data are observed at a resolution of 1 m or less. To properly down-sample or decimate the original data to 2 m or 10 m, we must remove noise and eliminate high frequency variation that the coarser destination resolution cannot represent. Decimation is supported by ArcGIS Terrain models when they are converted to a DEM—information is averaged or filtered over a "window." The effect on longitudinal and lateral profiles of using different window sizes for filtering is demonstrated in Figure 6-16.
5. **The standard (Nyquist) distance** for aggregation suggests the window size should be at least equal to the destination resolution. We found that a small additional amount of smoothing gave a visually more pleasing shape without losing longitudinal detail. We use this window size for our production work.

Figure 6-17 shows the longitudinal and lateral profiles derived from DEMs at different resolutions, in each case fixing the relative window size. Medium-fine resolution multidimensional models would probably have a discretization length of 10 to 15 m laterally and 40 m longitudinally for this region, certainly no finer than 10 m. Hence, our interpretation of Figure 6-17 is that a 10 m DEM not only captures the stable bathymetric features in this region, it is the finest (not coarsest) level of detail appropriate for the region.

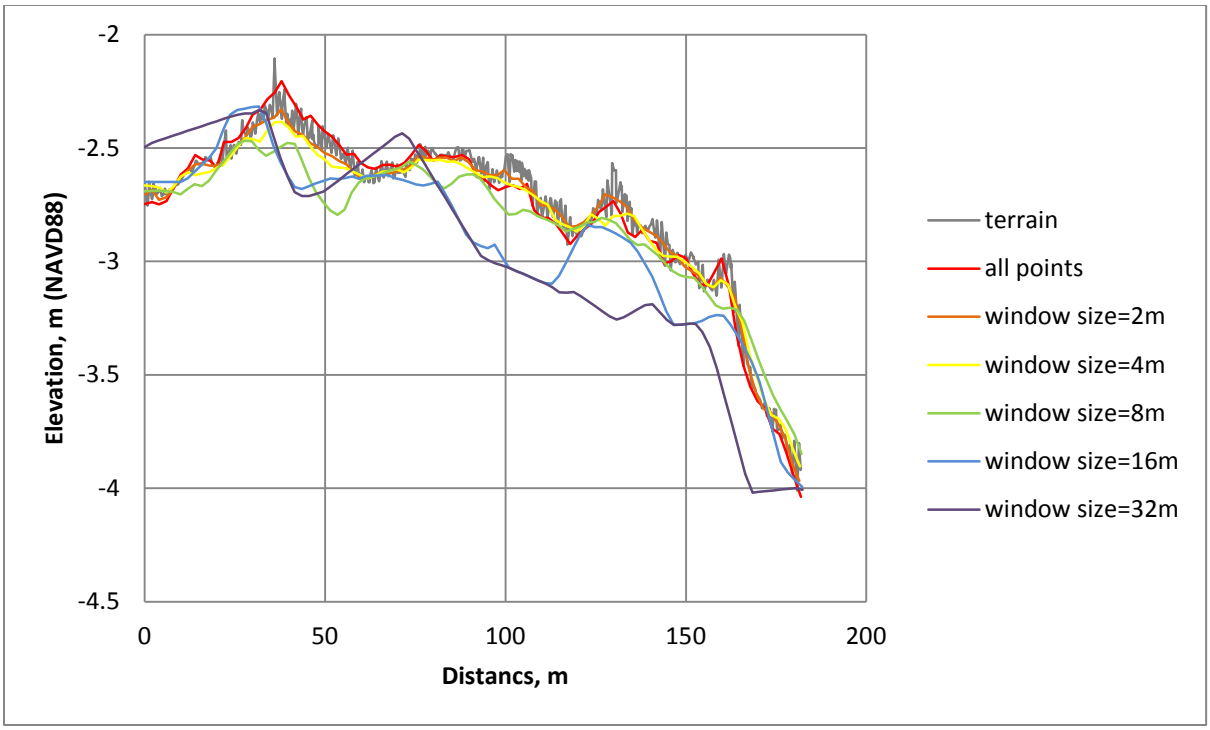

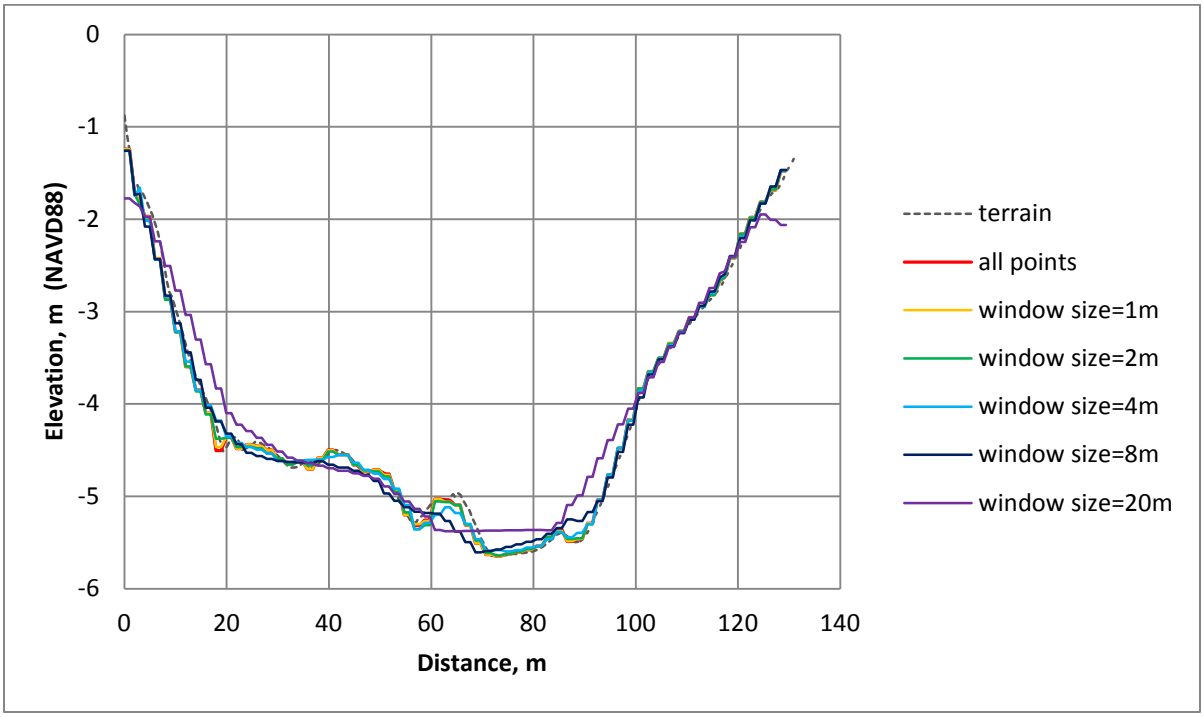

Figure note: The "window" size represents the extent over which averaging or aggregation is filtered.

Figure 6-16 Longitudinal Profile (top) and Lateral Profile for 2 m DEM Derived from Terrain Using Different Window Sizes

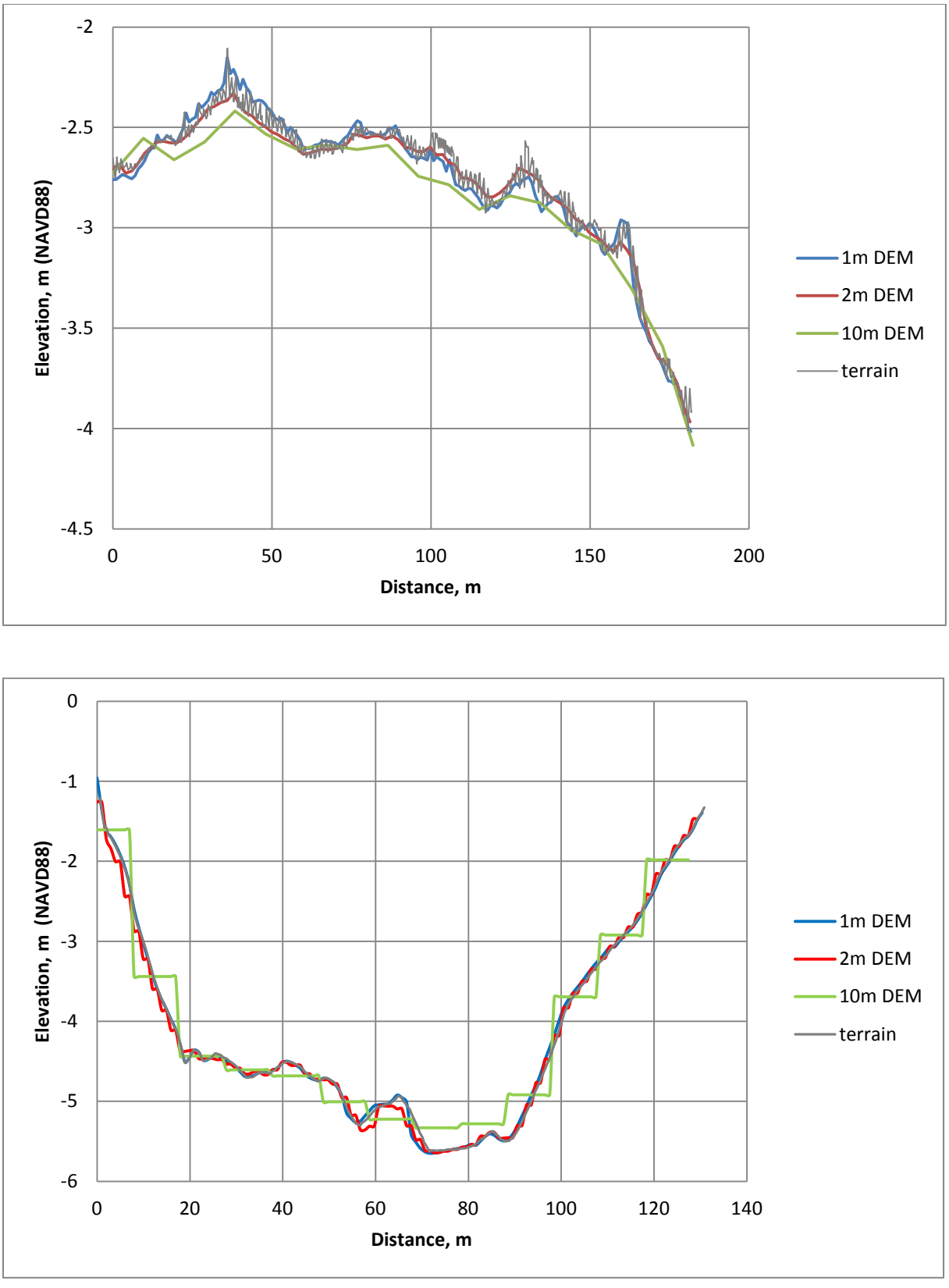

Figure 6-17 Longitudinal Profile (top) and Lateral Profile Generated from Different Resolution DEMs Using Same Proportional Window Size

6.8 Summary and Conclusions

Geometry is important to hydrodynamic models. In some locations, data used in the Bay-Delta is still in need of serious improvement. The authors have systemized the production of a 10 m/2 m elevation model for the Bay-Delta, borrowing strength from work done previously by the DWR, USGS, and NOAA and integrating new data when it becomes available. In many locations, the new geometry improves the quality of information we use in our hydrodynamic models, a point that will be amplified by the release of Version 2, which has many new sources of data. Some areas such as Mildred Island and the upper San Joaquin are still not well understood. The authors are hopeful that new soundings data will be collected before morphological change makes integration with LiDAR difficult.

The challenges of elevation mapping have changed since we began this work in 2010. Previously, our primary challenge was how to interpolate a realistic surface from sparse, poorly geo-referenced soundings often taken at intervals that seemed to have more to do with budget and technology than the scale of underlying features. Now, new data are over-resolved in space, and the quality of the integrated data set is determined by the handling of omissions and gaps. We are unaware of metrics for digital elevation models that are useful in the case where the distribution of error is concentrated in a small section of the tidal prism and where inundated area (for a given water surface) is quantified. We have some promising techniques for fixing the gaps in cases where out-of-the-box GIS techniques fail and where there is supporting data and aerial photography, which we will write about in a future report. However, the point of decreasing returns is easy to reach—good interpolants add realism and robustness to an elevation model, but they don't give new information.

Lastly, as resolution goes up, sampling frequency must be properly accounted for when a geographic elevation model is shaped into a bathymetry model for hydrodynamics. We have attempted to stage our products in such a way that we retain most of the detail of the raw data in our terrain models and point data, but correctly down-sampled products for applications.

We would like users to acquire our elevation model—and help criticize it! The data are distributed under a copyleft license with the understanding that we are interested in collaboration and improvement and improvements should be shared. Collaborators are asked to join our issue tracking system.

6.9 References

Campbell, C. (2012). Tule Canal and Toe Drain Bathymetry - Data Collection Procedures.

Carignan, K. S., Taylor, L. A., Eakins, B. W., Caldwell, R. J., Friday, D. Z., Grothe, P. R., et al. (2010). *Digital Elevation Models of Central California and San Francisco Bay: Procedures, Data Sources and Analysis.* NOAA Technical Memorandum NESDIS NGDC-52.

Casciola, G., Lazzaro, D., Montefusco, L. B., & Morigi, S. (2005). Fast surface reconstruction and hole filling using Radial Basis Functions. *Numerical Algorithms, 39*(1-3), 289-305.

Casciola, G., Lazzaro, D., Montefusco, L. B., & Morigi, S. (2006). Shape preserving surface reconstruction using locally anisotropic radial basis function interpolants. *Computers and Mathematics with Applications, 51(8)*, 1185-1198.

EDS [Environmental Data Solutions]. (2006). Draft Filed Data Report - Barker Slough, Calhoun Cut, Lindsey Slough and Cache Creek, Solano County, CA - Bathymetric Survey.

EDS [Environmental Data Solutions]. (2009). West Delta Condition Bathymetric Surveys: Field Data Collection Procedures. Prepared for cbec, Inc.

Foxgrover, A., Smith, R. E., & Jaffe, B. E. (2003). Suisun Bay and Delta Bathymetry: Production of a 10m Grid. *CALFED Science Conference.*

Fugro West, Inc. (2008). Bathymetric Surveys in Support of Urban Levees, Geotechnical Evaluation. Prepared for URS Corporation and California Department of Water Resources, DWR Task Order 32.

Fugro West, Inc. (2010). Multibeam Hydrographic Survey Middle River. Prepared for Storesund Consulting.

GRS [Global Remote Sensing LLC]. (2008). Mokelumne River (California Delta), California Hydrographic Survey Report. Prepared for the law offices of Herum Crabtree Brown.

HDR. (2011). Bathymetry Surveying in Support of Hydraulic Model Development Summary Report. DWR Task Order 18, Contract No. 4600007990, Lower San Joaquin River System.

Mayr, S. (2011). Multibeam Bathymetry Survey Report: Middle River - North Canal - Victoria Canal. Bathymetry and Technical Support Section, North Central Region Office, Division of Integrated Regional Water Management, California Department of Water Resources.

Merwade, V. M., Maidment, D. R., & Goff, J. A. (2006). Anisotropic considerations while interpolating river channel bathymetry. *Journal of Hydrology, 331(3-4)*, 731-741.

CSDP bathymetry data. (online). Retrieved from Bay-Delta Office, California Department of Water Resources: http://baydeltaoffice.water.ca.gov/modeling/deltamodeling/models/csdp/csdp.cfm

PBS&J, An Atkins Company. (2010). WR TO18 FINAL Technical Memo/Quality Control Report. DWR Task Order 18. Contract No. 4600007989, Lower Sacramento River Basin.

Ruggeri-Jensen-Azar & Associates. (2005). Grading Plans Subdivision 6013 – Delta Coves, Bethel Island, Contra Costa County, California, for DUC Housing Partners, Inc.

Smith, P. E. (n.d.). 10 m digitized bathymetry map. Sacramento, CA.

Towill, Inc. (2009). Sacramento DWSC 3D Models and San Francisco to Stockton DWSC 3D Models.

US Geological Survey. (2008). Northern Sacramento River Detailed Modeling Survey, Jun - 08 (online). Availability: https://sites.google.com/site/bathmapperwiki/Home/bathymetry-surveys/northern-sacramento-river-detailed-modeling-survey-june---07.

Wood, S. N. (2006). *General Additive Models.* Chapman and Hill.

Wood, S. N., Bravington, M. V., & Hedley, S. L. (2008). Soap film smoothing. *Journal of the Royal Statistical Society, Series B; 70*(5), pp. 931-935.